Supporting Information

Mechanically robust, self-reporting and healable polyurethane elastomers by incorporating symmetric/asymmetric chain extenders

Haitao Wu,[a] Hao Wang,[a] Mi Luo,[b] Zhaoyang Yuan,[a] Yiwen Chen,[b] Biqiang Jin,[a] Wenqiang Wu,[a] Bangjiao Ye,[b] Hongjun Zhang[b] and Jinrong Wu*[a]

[a] State Key Laboratory of Polymer Materials Engineering, College of Polymer Science and Engineering, Sichuan University, Chengdu, 610065, China

E-mail: wujinrong@scu.edu.cn (J. W.)

[b] State Key Laboratory of Particle Detection and Electronics, University of Science and Technology of China, Hefei 230026, China

Experimental Section

Materials

Polytetramethylene ether glycol (PTMEG, M_n=2000 g mol^{-1}) was purchased from Aladdin Chemical Reagent Co., Ltd. and was vacuum drying at 120 °C for 2 h to remove moisture before use. Other reagents without further purification before use. Isophorone diisocyanate (IPDI, 99%) and hydroxyl terminated polydimethylsiloxane (HO-PDMS-OH, M_n=4200 g mol^{-1}) were purchased from Shanghai TITAN Technology Co., Ltd (China). Hydrochloric acid (HCl), sodium hydroxide (NaOH), dibutyltin dilaurate (DBTDL, 95%), 4-aminophenyl disulfide (APDS), anhydrous tetrahydrofuran (THF, 99.5%), anhydrous dimethyl formamide (DMF, 99.8%), 2-(4-aminophenyl)-5-aminobenzimidazole (PABZ), N-hexane, hydrochloric acid (HCl) and sodium hydroxide (NaOH) were purchased from Adamas (China).

Synthesis of pre-polymer

PTMEG (14 g, 0.007 mol) and HO-PDMS-OH (4.20 g, 0.001 mol) were dissolved in 100 ml THF. Then, the solution containing PTMEG and HO-PDMS-OH was heated to 50 °C in an argon atmosphere. IPDI (3.56 g, 0.016 mol) and DBTDL (0.2 ml) were added to the solution. This solution was continuously stirred at 50 °C for 24 h to obtain the pre-polymer solution.

Synthesis of the PU elastomer

For the synthesis of the PU elastomer, PABZ (0.90 g, 4.00 mmol) was firstly added into the pre-polymers (22.74 g, 8.00 mmol) solution, and the solution was stirred at 60 °C for 24 h in an argon atmosphere. Secondly, APDS (0.99 g, 4.00 mmol) was charged into the above solution. The resulting solution was heated to 60 °C and continuously stirred in an argon atmosphere for 24 h. Subsequently, the reaction solution was poured into n-hexane (500 ml) to precipitate the product and washed three times. Finally, the precipitate was dried under vacuum for 24 h to obtain the PU elastomer (20.5 g, 83.3%).

A series of the PU elastomers were synthesized by tuning the molar ratio of chain extenders (APDS and PABZ). The feed ratios of the PU-X/Y elastomer (X and Y denote the molar ratio of chain extenders APDS and PABZ, respectively) are summarized in Table S1 (ESI).

Fabrication of the PU elastomer film

The PU elastomer film was fabricated by casting a THF solution of the PU onto a cleaned Teflon mold (100 × 100 × 10 mm). The PU sample solution was gradually dried under room temperature over 24 h, followed by heating at 60 °C for another 12 h and peeling off the elastomer films from the Teflon mold.

Characterizations

All the PU samples were vacuum-dried at 50 ℃ for 12 h before characterizations. Gel permeation chromatography (GPC) analysis was performed to characterize the molecular weight and its distribution of the PU samples. The X-ray electron diffraction energy spectrometer (EDS, INCA250 Oxford Instruments, UK) was used to prove the existence of disulfide bonds in the PU samples.

Attenuated total reflectance (ATR) mode-Fourier transform infrared (FTIR) spectrum

ATR-FTIR (Thermo Nicolet-is50) was used to characterize the molecular structure of the PU samples at room temperature. The test was performed with 32 scan times in a range of 4000-800 cm^{-1}. Variable-temperature FTIR spectra were recorded in the temperature ranging from 40 to 150 °C with a heating rate of 5 °C min^{-1}.

Dynamic thermomechanical analysis (DMA) tests

DMA (TA Instruments Q800) were performed to characterize the network relaxation of the PU samples. Mechanical properties test was performed on a universal testing machine (USA, Instron Instruments, model: 5967).

Mechanical properties measurements

Mechanical properties of the PU samples were measured with a universal testing machine (USA, Instron Instruments, model: 5967), and the tensile speed 50 mm min^{-1}. Each sample was tested three times. Cyclic tensile test was performed by conducting successive loading-unloading cycles with a maximum strain of 700%. Self-healing test was performed: the dumbbell spline with 0.7 mm thick was cut two parts by means of fresh blade, immediately spliced together to investigate the healing ability at different time and temperatures.

Optical microscope (DM4P/Leica, Germany)

Scratch recovery process was observed by an optical microscope equipped with a hot stage at different time.

Situ wide-angle X-ray diffraction (WAXD) measurement

In situ synchrotron WAXD measurements were performed at the beamline BL16B1 in Shanghai synchrotron radiation facility (SSRF), China. A wavelength of 0.124 nm was used and the two-dimensional (2D) WAXD patterns were recorded by MAR-CCD detector. The stretching machine used in the measurement was the Linkam TST350 tension machine. The exposure time for each pattern was varied according to the stretching rates, i.e. 30 s for 0.002 s^{-1},10 s for 0.01 s^{-1} and 5 s for 0.05 s^{-1}. The diffraction angle in WAXD was calibrated by the CeO2 standard. The WAXD patterns were background corrected and processed using Fit2D software for further analysis. These corrected WAXD patterns were integrated along the azimuthal direction from 0° to 180°.

Small angle X-ray scattering (SAXS) measurement

In SAXS measurements were performed at the beamline BL16B1 in Shanghai synchrotron radiation facility (SSRF), China. The wavelength of X-ray is 0.124 nm, the distance from the sample to the detector is 1360 mm. The SAXS patterns were

processed using Fit2D software for further analysis.

Density functional theory (DFT) calculations

DFT calculations were performed using Gaussian 16 suite of programs and data analysed using multiwfn_3.7_bin_win64 software. All structures were fully optimized at the M06-2X/6-311+g (d, p) // B3LYP/6-311+ g (d, p) level. To prove the formation of disorder hard domains in the PU elastomer, small molecule models were used to perform DFT calculations (Figure S17). Firstly, B3LYP/6-311+g (d, p) level was utilized for geometric configuration optimization and frequency calculation of small molecule models. Subsequently, M06-2X/6-311+g (d, p) level was used to describe the conformational change caused by the weak interactions (π-π stacking and H-bonds) of small molecule models. Meanwhile, the keyword "counterpoise" was used to correct the basis-set superposition error (BSSE). Herein, we select the dimers and tetramers of chain extenders (APDS and PABZ) serve as small molecular models to reflect the aggregation state of hard domains. The molecular structure after configuration stabilization as shown in Fig. 1(f), Fig. 2(g) and Figure S5. Clearly, a regular topology structure can be formed for dimers (APDS-dimers and PABZ-dimers) and tetramers (APDS-tetramers and PABZ-tetramers) due to the existence of weak interactions (π-π stacking and H-bonds) between small molecule models. Meanwhile, the dimers or tetramers of APDS-PABZ show the most irregular molecule conformations. Thus, this DFT calculations results reveal that the formation of disordered hard domains in the PU system.

Calculation of interaction energies. The interaction energy (ΔE) is expressed by the energy difference between the complex ($E_{\text{APDS-APDS}}$, $E_{\text{APDS-PABZ}}$ and $E_{\text{PABZ-PABZ}}$) and the chain extender monomers (E_{APDS} and E_{PABZ}). Firstly, optimizing the monomers (APDS and PABZ) geometric structure and frequency calculation at B3LYP/6-311+g (d, p) level to obtain the thermodynamic energy correction value and zero-point energy correction (ZPEC). Secondly, optimizing the $E_{\text{APDS-APDS}}$, $E_{\text{APDS-PABZ}}$ and $E_{\text{PABZ-PABZ}}$ and APDS and PABZ geometric structure and frequency calculation at M06-2X/6-311+g (d, p) level. Meanwhile, the keyword "counterpoise" was used to correct the basis-set

superposition error (BSSE). Therefore, the different interaction energies are calculated:

$$\Delta E = E_{complex} - E_{APDS} - E_{PABZ} + BSSE$$

where $E_{complex}$, E_{APDS}, E_{PABZ} and BSSE are the complex (E_{AB}) energy, monomer APDS (total electronic energy), monomer PABZ (total electronic energy) and basis-set superposition error correct value, respectively.

All-atom molecular dynamics (MD) simulations

All-atom molecular dynamics (MD) simulations were performed using the Amorphous Cell and Forcite module of the Materials Studio (MS 2020 version). The simulated systems comprise five polymer chains, and each polymer chain consists of four hard and five soft segments. The number of repeating units in the soft segments are 12. In the simulation process, the cubic box size is 33×33×33 Å and three-dimension (3D) periodic boundary conditions in three directions are used. All of the units were placed in a simulated cubic box to reflect the actual molecular chain configuration. The initial configurations were constructed by randomly distributing the polymer chains in simulation cells using the Amorphous Cell module of the Materials Studio (MS 2020 version). The condensed-phase optimized molecular potentials for atomistic simulation studies (COMPASSII) force field was selected to describe the interactions in the polymer chains. The amorphous cells were optimized by the Smart Minimized method. After that, the Forcite module was used to calculate the equilibrium configurations of polymer chains and the cohesive energy of the networks. Specifically, the cells were further annealed between 300 K and 500 K for 10 circles with 10 heating ramps per circle. Then, MD simulation was carried out for 300 ps NVT (keep the number of atoms, volume and temperature constant) at 298 K and 500 ps NPT (keep the number of atoms, pressure, and temperature constant) at 298 K and 0.0001 GPa to obtain the equilibrium density. Another 500 ps NVT was carried out at a reasonable density to obtain the most stable configuration. During the calculation process, the Berendsen Barostat and Andersen Thermostat were chosen for controlling the pressure and temperature,

respectively[1]. Ewald and Atom-based were chosen as the calculation methods for electrostatic and van der Waals interactions.

Calculation of the cohesive energy. The cohesive energy per chain is defined as the average energy per chain required to separate all the polymer chains in a condensed state into infinite distance from each other. In the PU elastomer systems, the cohesive energy per chain was calculated by the following equation:[1]

$$E_{cohesive} = \frac{\left(\sum_{i=1}^{5} E_{pot}^{isolated}(i) - E_{pot}^{5}\right)}{5}$$

where $E_{pot}^{isolated}$ is the average potential energy of an isolated polymer chain in vacuum, and E_{pot}^{5} is the average potential energy of the condensed system consisting of five polymer chains. The potential energies of the isolated polymer chains are calculated by averaging 20 frames in 100 ps after the equilibrium simulation of 1000 ps. For the condensed system, the potential energy was calculated via the same method after the annealing simulation.

Positron annihilation lifetime spectroscopy (PALS) test

PALS were collected by a conventional fast-fast coincidence system with a time resolution (free width at half maximum, FWHM) of ~210 ps at room temperature. The positron source (^{22}NaCl, sealed between two polyimide Kapton supporting foils in the size of 10 mm×10 mm×7.5 μm) was sandwiched between two identical samples with dimensions of 10×10×1 mm. The start and stop signals (γ rays of around 1.28 and 0.511 MeV, respectively) were collected by two detectors. To prevent backscattering of γ rays, the two detectors were perpendicularly positioned. The distance between the sample-source-sample set and the two lifetime detectors was around 20 mm. The total count of each PALS was 2.0 x 10^6, with a count rate of around 300 counts/s. The source correction (positron annihilation in ^{22}NaCl and two polyimide Kapton supporting foils) was determined by the measurement of two identical YSZ (ZrO) samples in the size of 10×10×1 mm.

Each lifetime spectrum can be resolved into three lifetime components using LTv9 program. The short-lived component (lifetime 1, τ_1) and the intermediate-lived component (lifetime 2, τ_2) correspond to the para-positron (*p*-Ps). The longest life component (lifetime 3, τ_3), which is the pick-off annihilation of positron (*o*-Ps). The lifetime and intensity of *o*-Ps are directly related to the size and number of free-volume hole within polymer bulk. Using the Tao-Eldrup model,[2] the average radius (R) of the free-volume holes could be estimated from the *o*-Ps lifetime τ_3:

$$\tau_3^{-1} = 2\left[1 - \frac{R}{R+\Delta R} + \frac{1}{2\pi}\sin\left(2\pi\frac{R}{R+\Delta R}\right)\right] \quad (1)$$

where ΔR corresponds to the thickness of the electron layer on the surface of the free-volume holes, which is an empirical value (0.1656 nm) for polymers.

The average size of free-volume holes (v_f) could be estimated:

$$v_f = 4\pi R^3/3 \quad (2)$$

The relative fraction free volume f_r (%) is defined as:

$$f_r = v_f I_3 \quad (3)$$

where I_3 is *o*-Ps intensity.

Proton multiple-quantum (MQ) test

Proton double-quantum (DQ) spectra were collected to probe segmental dynamics of the PU samples. Specimen preparation process: specimens were cut into small pieces, and then put into the NMR tube (10 mm outer diameter) with a height of around 1 cm sample. Proton MQ tests were performed on a Bruker Minispec mq20 at 20 MHz proton resonance frequency. The Minispec has a typical π/2 pulse length of about 2.75 μs and a receiver dead time of about 8.6 μs. Two sets of data can be obtained from the MQ NMR experiment with evolution in the DQ excitation/reconversion time, corresponding to the signal intensity of double-quantum (DQ) coherences (I_{DQ}) and the reference intensity (I_{ref}), respectively. DQ signal intensity will undergoes the relaxation

at a long evolution time, and thus require a point-to-point normalization protocol[3] to acquire a normalized DQ buildup intensity as a function of DQ evolution time (τ_{DQ}). Before normalization, however, the slowly relaxed isotropic flexible component signals (such as the dangling chains in polymers) which have no contribution to the DQ signals must be subtracted from the MQ signals. These segments show as a slow decaying tail in the curve of $I_{ref}(\tau_{DQ}) - I_{DQ}(\tau_{DQ})$.

$$I_{nDQ}(\tau_{DQ}) = \frac{I_{DQ}(\tau_{DQ})}{I_{ref}(\tau_{DQ}) + I_{DQ}(\tau_{DQ}) - I_{tail}(\tau_{DQ})} \qquad (4)$$

Fracture Energy

The fracture energy was calculated by Greensmith method,[4] the specific calculation formula is following as:

$$G_c = \frac{6WC}{\sqrt{\lambda_c}} \qquad (5)$$

where C is the notch length; W is the strain energy calculated by integration of the stress-strain curve of an un-notched sample until λc; the un-notched sample undergoes a tension λc process with the same strain rate as the notched sample. In this test, the tensile speed was 3 mm min^{-1}.

Fluorescence spectrometer test

Fluorescence spectra of the PU samples were measured by the fluorescence spectrometer (HORIBA company, Japan). Meanwhile, the normalized fluorescence intensity changes of the PU samples during stretching were studied with a homemade small tensile machine at fixed stain of 20%. Specific normalization procedure of fluorescence intensity at a fixed strain of 20% is following as:

$$I = \frac{I_0}{I_t} \qquad (6)$$

where I_0 is the original fluorescence intensity at a fixed strain of 0%, I_t is the fluorescence intensity of different time at fixed strain of 20%.

Pre-fabrication of chemical damage

Firstly, prepare a solution of hydrochloric acid (HCl) and sodium hydroxide (NaOH) at a concentration of 1 M. Tetrahydrofuran (THF) is chosen as the solvent due to the hydrophobicity of the PU elastomers. Secondly, the prepared strong HCl and NaOH solutions were dropped onto the surface of the PU elastomers using a dropper, respectively, causing disruption of the network structure of the samples and changes in fluorescence intensity. Finally, the healing process was visualized by observing the change in fluorescence intensity.

Supplementary Tables

Table S1. Feed ratios used in the synthesis of the PU elastomers.

Sample	PTMEG (g) (2000 g mol^{-1})	OH-PDMS-OH (g) (4200 g mol^{-1})	APDS (g)	PABZ (g)	IPDI (g)	DBTDL (ml)	M_n (x10^4 g mol^{-1})	PDI
PU-1/9	14	4.2	0.20	1.61	3.56	0.2	9.9180	1.83
PU-2/8	14	4.2	0.40	1.44	3.56	0.2	10.0764	1.84
PU-5/5	14	4.2	0.99	0.90	3.56	0.2	9.4743	1.76
PU-8/2	14	4.2	1.59	0.36	3.56	0.2	10.7557	1.85

Table S2. Summary of the mechanical properties of the PU elastomers.

Sample	Mechanical strength (MPa)	Fracture strain (%)	Young's modulus (MPa)	Toughness (MJ m^{-3})
PU-1/9	49.12±3.40	949.10±20.33	7.40±0.05	124.14±5.31
PU-2/8	45.24±2.55	887.80±30.51	12.70±0.20	100.49±2.54

PU-5/5	60.70±3.74	1170.47±36.55	13.10±0.10	177.85±8.23
PU-8/2	51.96±3.13	874.10±26.48	13.40±0.30	120.38±6.87

Supplementary Figures

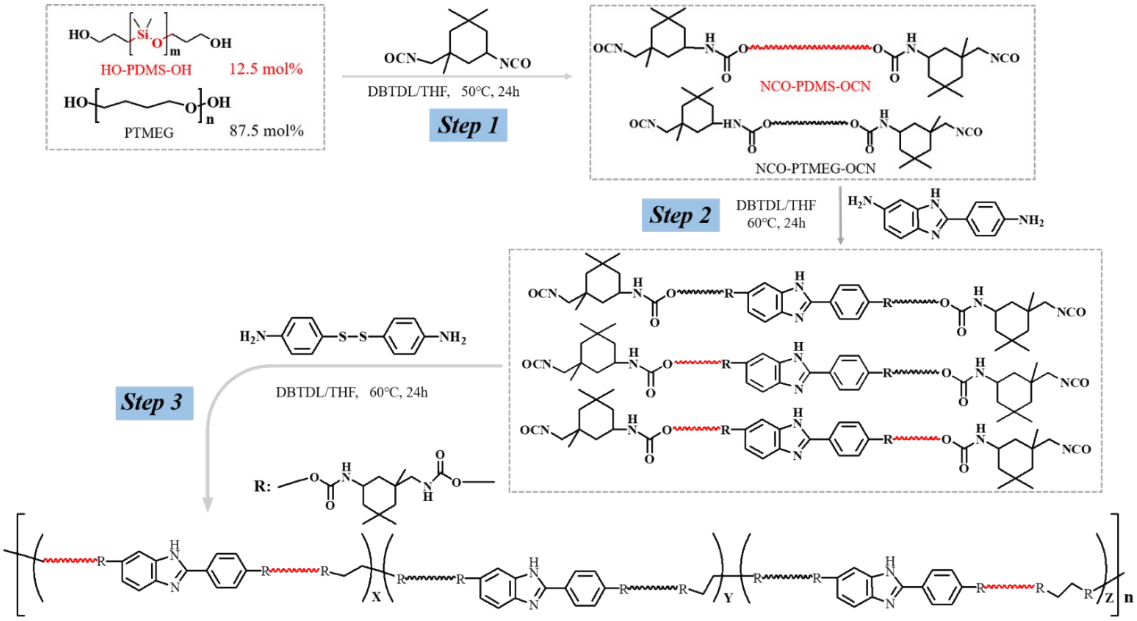

Fig. S1 Synthesis route of resulting PU elastomer.

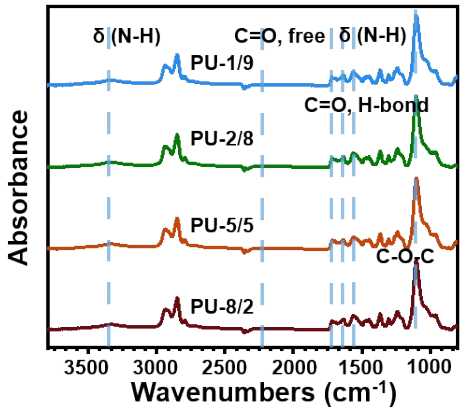

Fig. S2 The ATR-FTIR spectra of obtained PU elastomers in the region 4000-800 cm-

As seen, ATR-FTIR of all the PU elastomers feature negligible peaks at 2258 and 3458 cm^{-1}, corresponding to the stretching vibrations of the N=C=O and O–H, respectively.[1] suggests that the isocyanate and hydroxyl groups are fully converted to urethane bonds. Simultaneously, some characteristic peaks of these polymers were observed. The obvious peaks at around 3343 cm^{-1} and 1557 cm^{-1} should be ascribed to the N-H stretching vibration and bending vibration of N-H, respectively.[5] Characteristic absorption peaks at 1717 cm^{-1} and 1629 cm^{-1} should be assigned to the C=O stretching vibration of urea and urethane groups, respectively.[1] These results suggest the hydrogen bonds formed by urea and urethane groups are successfully introduced into the polymers.

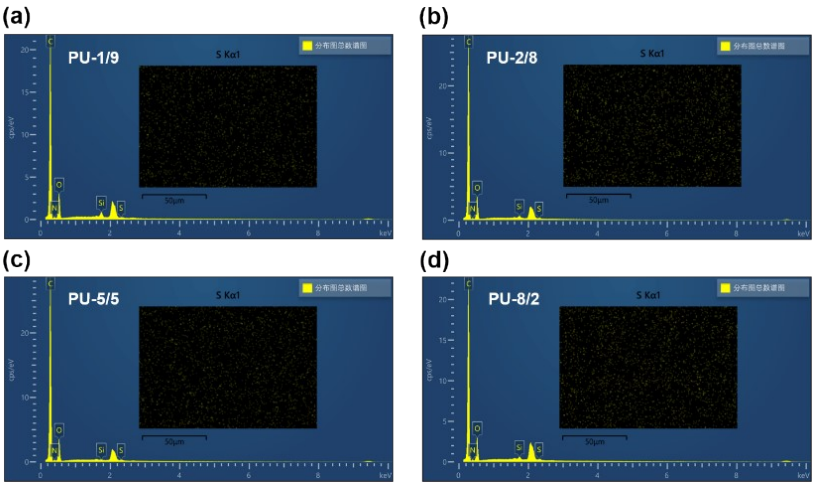

Fig. S3 The X-ray electron diffraction energy spectra (EDS) of obtained PU elastomers.

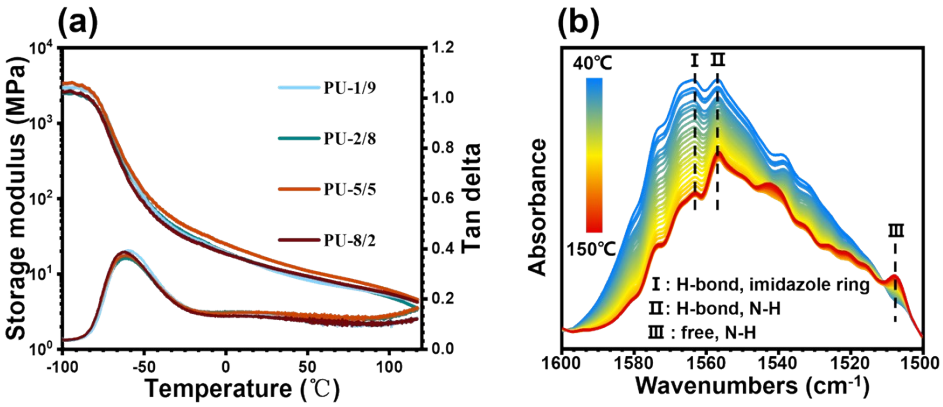

Fig. S4 (a) Dynamic mechanical analysis (DMA) spectra of the PU elastomers to determine the glass transition temperature (T_g). (b) Temperature-dependent FTIR spectra at 1500-1600 cm^{-1} in the N-H region upon heating from 40 to 150 ℃.

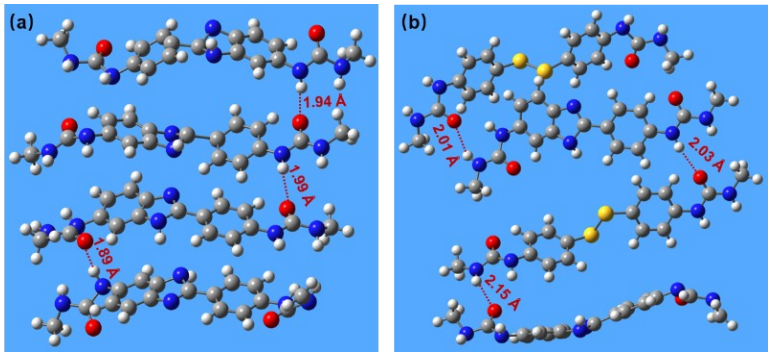

Fig. S5 Optimal conformations of tetramers of (a) PABZ and (b) APDS-PABZ.

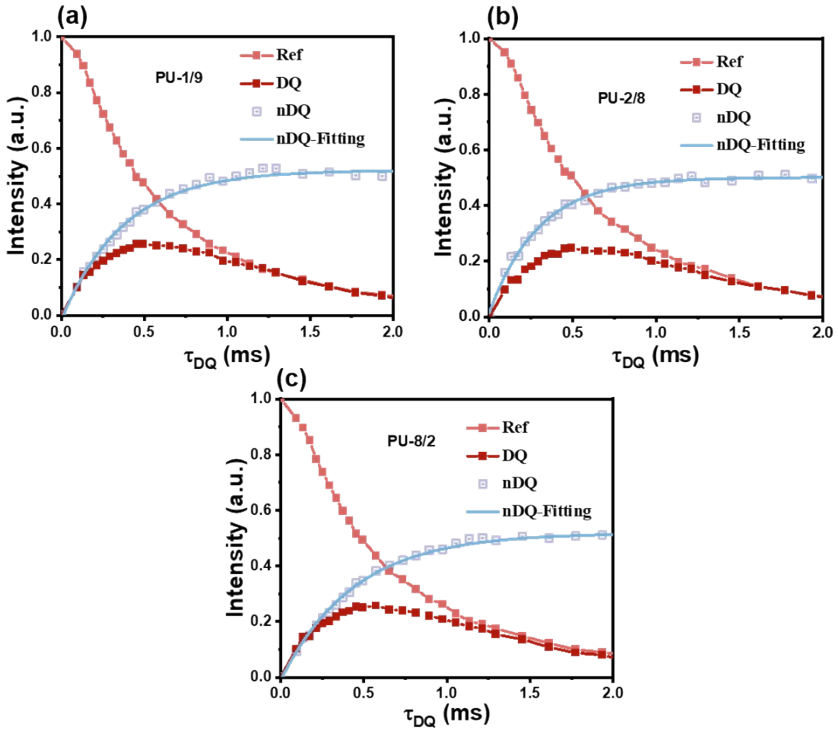

Fig. S6 Obtained double-quantum (DQ) intensity and reference signal decay as a function of DQ excitation time for (a) PU-1/9, (b) PU-2/8 and (c) PU-8/2.

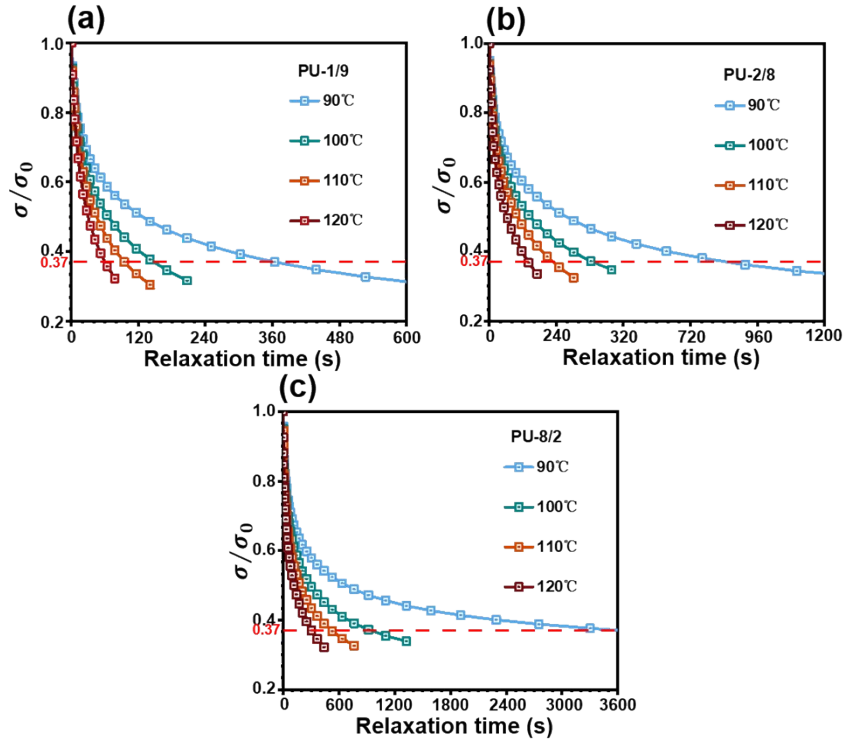

Fig. S7 Varied-temperature stress relaxation spectra of (a) PU-1/9, (b) PU-2/8 and (c)

PU-8/2.

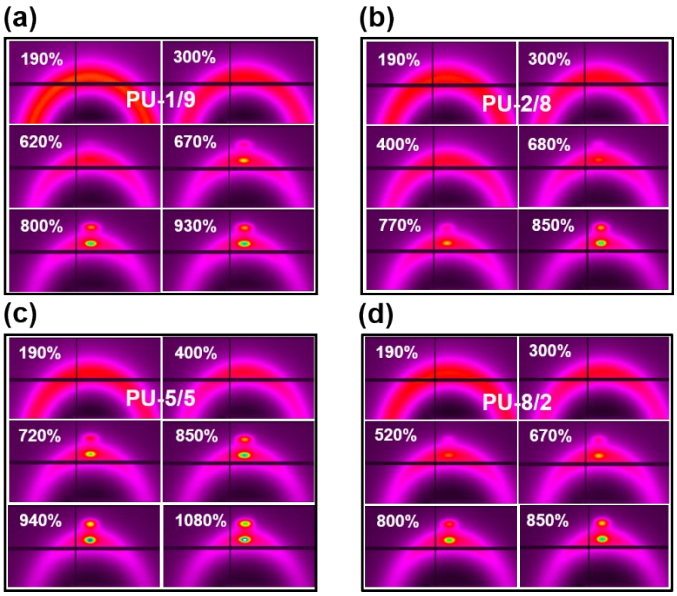

Fig. S8 Two-dimensional (2D) wide-angle X-ray diffraction (WAXD) patterns at different strains for all the PU elastomers.

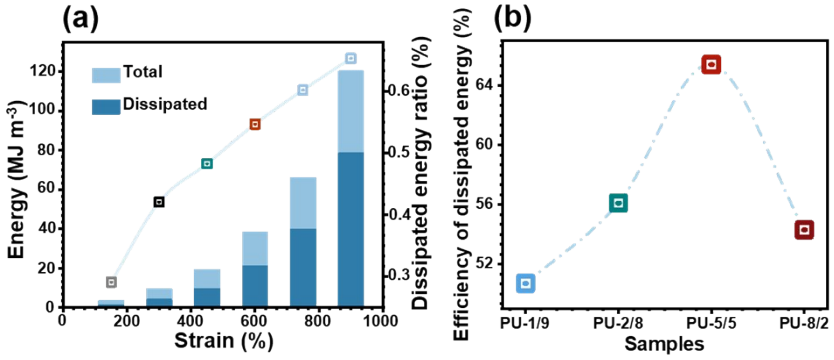

Fig. S9 (a) Dissipated energy and ratio at each loading-unloading cycle of the PU-5/5 elastomer. (b) Summary of efficiencies of dissipated energy for all the PU elastomers.

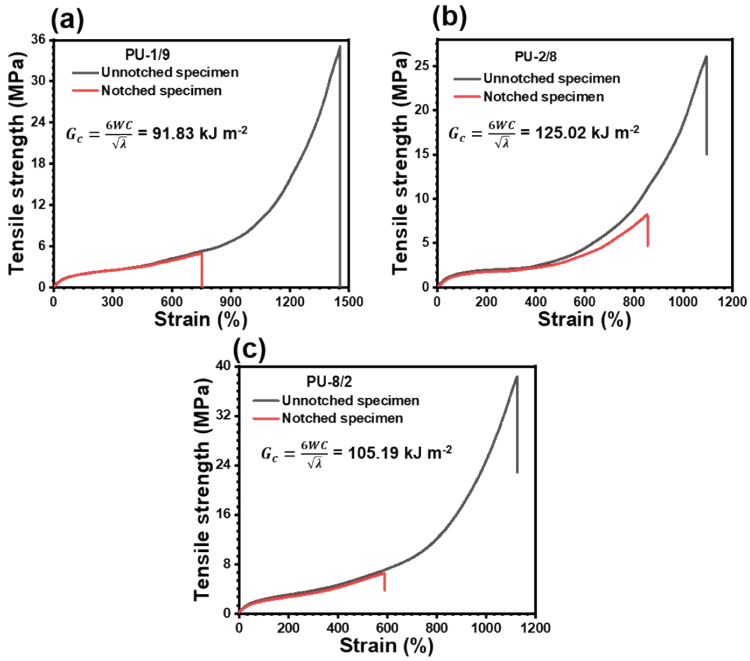

Fig. S10 Fracture energies of (a) PU-1/9, (b) PU-2/8 and (c) PU-8/2.

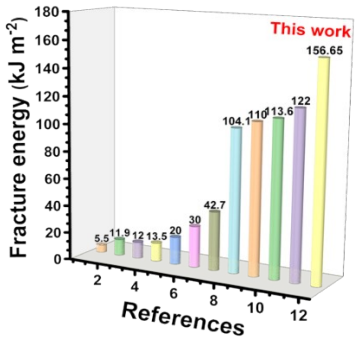

Fig. S11 Comparing the fracture energy of the PU-5/5 to previously reported healable and unhealable materials.[4,6–14,15]

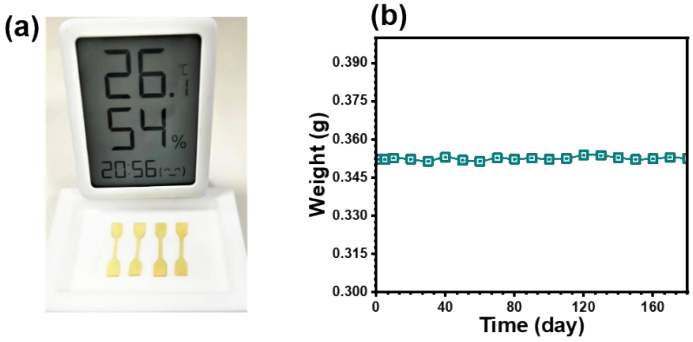

Fig. S12 (a) Monitoring of the temperature and relative humidity. (b) Weight change of the PU-5/5 in a humid environment with a temperature of 26 ℃ and a relative humidity of 54% for six months.

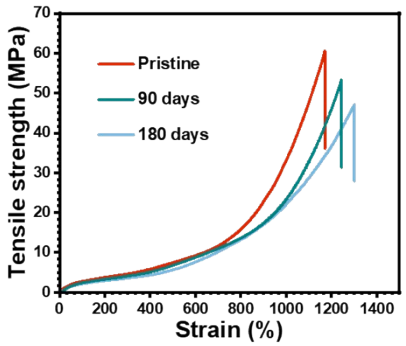

Fig. S13 Variation of mechanical properties of the PU-5/5 in humid environment with a temperature of 26 ℃ and a relative humidity of 54% for 180 days.

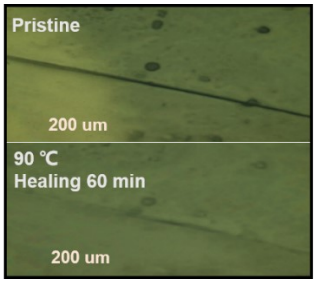

Fig. S14 Optical microscopy images of the scratched PU-5/5 film in healing process at 90 ℃.

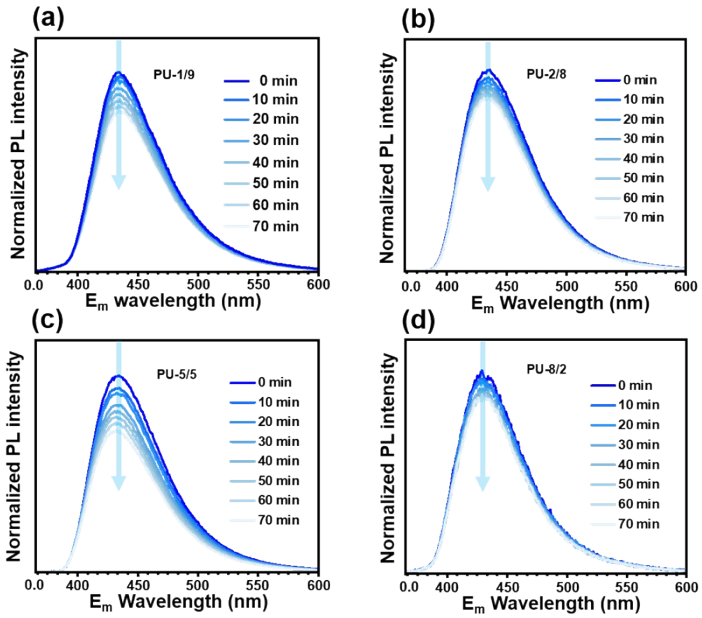

Fig. S15 Changes in fluorescence intensity during the network relaxation process of all the PU elastomers.

References

1 Z. Li, Y. L. Zhu, W. Niu, X. Yang, Z. Jiang, Z. Y. Lu, X. Liu and J. Sun, *Adv. Mater.*, 2021, **33**, 2101498.

2 S. J. Tao, *J. Chem. Phys.*, 1972, **56**, 5499–5510.

3 R. Zhang, C. Zhang, Z. Yang, Q. Wu, P. Sun and X. Wang, *Macromolecules*, 2020, **53**, 5937–5949.

4 Y. Li, W. Li, A. Sun, M. Jing, X. Liu, L. Wei, K. Wu and Q. Fu, *Mater. Horiz.*, 2021, **8**, 267–275.

5 Y. Wang, X. Huang and X. Zhang, *Nat. Commun.*, 2021, **12**, 1291.

6 D. Wang, J. H. Xu, J. Y. Chen, P. Hu, Y. Wang, W. Jiang and J. J. Fu, *Adv. Funct. Mater.*, 2020, **30**, 1907109.

7 J. Kang, D. Son, G. J. N. Wang, Y. Liu, J. Lopez, Y. Kim, J. Y. Oh, T. Katsumata, J. Mun, Y. Lee, L. Jin, J. B. H. Tok and Z. Bao, *Adv. Mater.*, 2018, **30**, 1706846.

8 L. Chen, T. L. Sun, K. Cui, D. R. King, T. Kurokawa, Y. Saruwatari and J. P. Gong, *J. Mater. Chem. A*, 2019, **7**, 17334–17344.

9 C. Jin, G. Sinawang, M. Osaki, Y. Zheng, H. Yamaguchi, A. Harada and Y. Takashima, *Polymers*, 2020, **12**, 1393.

10 S. Chen, L. Sun, X. Zhou, Y. Guo, J. Song, S. Qian, Z. Liu, Q. Guan, E. Meade Jeffries, W. Liu, Y. Wang, C. He and Z. You, *Nat. Commun.*, 2020, **11**, 1107.

11 W. Cui, D. R. King, Y. Huang, L. Chen, T. L. Sun, Y. Guo, Y. Saruwatari, C. Y. Hui, T. Kurokawa and J. P. Gong, *Adv. Mater.*, 2020, **32**, 1907180.

12 J. Li, W. R. K. Illeperuma, Z. Suo and J. J. Vlassak, *ACS Macro Letters*, 2014, **3**, 520–523.

13 Y. Wang, X. Liu, S. Li, T. Li, Y. Song, Z. Li, W. Zhang and J. Sun, *ACS Appl. Mater. Interfaces*, 2017, **9**, 29120–29129.

14 M. Vatankhah-Varnosfaderani, A. N. Keith, Y. Cong, H. Liang, M. Rosenthal, M. Sztucki, C. Clair, S. Magonov, D. A. Ivanov, A. V. Dobrynin and S. S. Sheiko, *Science*, 2018, **359**, 1509–1513.

15 J. Hu, R. Mo, X. Jiang, X. Sheng and X. Zhang, *Polymer*, 2019, **183**, 121912.